**Communications in Mathematics and Applications**
Vol. 16, No. 4, pp. 1119–1129, 2025
ISSN 0975-8607 (online); 0976-5905 (print)
Published by RGN Publications
DOI: 10.26713/cma.v16i4.3323

http://www.rgnpublications.com

Research Article

# The Role of Hybrid Cu–Ag Nanoparticles in Modifying Blood Flow Through Narrowed Arteries

Nitin Sadashiv Bodke[1] and Ignatius Fernandes*[2]

[1] *Dr. B. N. Purandare, Arts, Smt. S. G. Gupta Commerce and Smt. S. A. Mithaiwala Science College, Lonavala 410403, Maharashtra, India*
[2] *Government College of Arts, Science and Commerce (affiliated to Goa University), Quepem, Goa, India*
***Corresponding author:** ignatius@gcq.ac.in

**Received:** August 16, 2025 **Revised:** November 10, 2025 **Accepted:** November 20, 2025

**Abstract.** Blood flow in stenosed human arteries in the presence of hybrid Copper-Silver (Cu–Ag) nanoparticles is studied. The study investigates the influence of copper (Cu) nanoparticles and Cu–Ag hybrid nanoparticles on velocity profiles, flow rate and resistive impedance to blood flow in abnormally narrowed arteries due to stenosis. A laminar unsteady blood flow is considered through a cylindrical tube depicting blood flow in an artery affected by stenosis. Flow parameters are assumed to match the physical properties of the blood flow. Finite difference method is employed to discretize the governing equations and simulation is carried out using MATLAB. The presence of hybrid nanoparticles is observed to have significant influence on velocity, flow rate and impedance to blood flow.

**Keywords.** Hybrid nanoparticles, Stenosed arteries, Copper-Silver nanoparticles

**Mathematics Subject Classification (2020).** 76Z05



## 1. Introduction

Nanoparticle drug delivery has rapidly become a transformative tool in the treatment of various diseases within the field of medical advancements. Nanomedicine, which lies at the intersection of nanotechnology and healthcare, focuses on the precise and controlled delivery of nanoscale materials to specific targets. This innovative approach holds significant promise, particularly in improving the efficacy of natural bioactive compounds. Atherosclerosis, a common cardiovascular

condition, arises from the accumulation of fatty deposits in the arteries, leading to blood flow disruptions—a condition known as stenosis. This contributes to cardiovascular disorders, which remain a leading cause of mortality worldwide. Consequently, a key area of research is centered on investigating the effects of nanoparticles on blood flow through stenotic regions, addressing an essential aspect of modern medical studies.

Many researchers have carried out research in the field of fluid flow in stenotic arteries when the fluid is augmented by nanofluids. Sarwar and Hussain [18] examined the influence of blood flow through a cosine-shaped stenotic artery in the presence of hybrid nanoparticles. In this study, blood flow is modeled as a Newtonian fluid, and a two-dimensional flow assumption is applied. The governing equations are formulated and solved using similarity transformation, taking into account the stenosis conditions. The study by Abbas *et al*. [1] analyzed blood flow containing nanoparticles through stenosed arteries, revealing that liquid velocity and flow rate increase with slip velocity and Womersley's frequency, while Lorentz force decreases them and body acceleration enhances fluid velocity, impacting overall flow dynamics. Muthtamilselvan and Hingis [12] considered gold nanoparticles for their study and observed that these nanoparticles enhance blood flow in stenotic arteries by emitting heat, which regulates the axial velocity of the flow. The study analyzed various physical parameters, demonstrating the nanoparticles' positive impact on blood flow dynamics in catheterized arteries with stenosis. The study presented by Raju *et al*. [16] focused on analyzing the flow of Sutterby gold blood nanofluid in two distinct stenotic arteries under the influence of periodic body acceleration. In this study, the Sutterby rheology model is considered representative of blood, and a single-phase model is employed to characterize the behavior of the nanofluid. The dimensional non-linear *partial differential equations* (PDEs) governing the system are transformed into dimensionless PDEs using non-similar variables. A finite-difference method is applied to solve these dimensionless PDEs. The impact of key flow parameters on the Sutterby nanofluids velocity, temperature, resistance impedance, flow rate, and wall shear stress is illustrated through graphical representations. Akbar *et al*. [3] examined the impact of magnetic forces and variously shaped nanoparticles on blood flow in diverging tapering arteries with stenoses, using a blood flow model. Algehyne *et al*. [4] investigated the unsteady sensitivity analysis and entropy generation in the flow of blood containing silver and titanium dioxide nanoparticles within a tilted cylindrical artery featuring a symmetric W-shaped stenosis. The study incorporates factors such as the electric field, Joule heating, viscous dissipation, and heat source while considering two-dimensional pulsatile blood flow and periodic body acceleration. The governing equations are solved using finite difference method.

Motlagh and Deyhim [11] studied magnetic drug targeting using $Fe_3O_4$ nanoparticles. The authors used a finite volume method for solving governing equations numerically. Badfar *et al*. [6] explored the numerical investigation of *Magnetic Drug Targeting* (MDT) within a stenotic blood vessel using a nanofluid containing drug-coated $Fe_3O_4$ nanoparticles. The authors applied the finite volume method to discretize the equations governing unsteady two-phase flow. The study by Sarwar and Hussain [18] investigated the impact of nanoparticles on the blood flow of a Jeffrey fluid in a tapered artery with stenosis. It considered slip effects and the permeable nature of the arterial wall, considering convection. Hussain *et al*. [8] used *Computational Fluid Dynamics* (CFD) analysis in COMSOL to study blood flow in abdominal aortic aneurysm. Blood is considered as the base fluid with $Fe_3O_4$ nanoparticles. The study focused on analyzing the flow characteristics of blood to assess the impact on pressure, velocity, and temperature due to an abdominal aortic aneurysm. The effect of Copper (Cu) and Silver (Ag) nanoparticles

on blood flow in stenosed arteries with aneurysm is studied by Zaman *et al*. [22]. In the study by Tang *et al*. [20] the flow of Sisko nanofluid, which included gold (Au NPs) through porous stenosed arteries was examined. Blood served as the base particle for the nanoparticles, and the study focused on exploring heat transfer properties with consideration for viscous dissipation. Waqas *et al*. [21] examined the significance of gold and silver nanoparticles immersed in human blood under the influence of *magnetohydrodynamics* (MHD) flow within a stenotic artery. Rehman *et al*. [15] examined the effects of nanoparticles for the blood flow of Jeffrey fluid in tapered artery with stenosis by taking into account the slip effects along with permeable nature of the arterial wall.

The comparative study of blood flow properties in stenosed region with the insertion of Copper (Cu) and Copper-Silver (Cu–Ag) hybrid nanoparticles has not been studied in the literature. In the present study, blood flow dynamics in the presence of Copper (Cu) and Copper-Silver hybrid (Cu–Ag) nanoparticles are explored.

## 2. Governing Equations

The stenosed artery segment, depicted in Figure 1, is conceptualized as a cylindrical tube carrying Newtonian fluid to represent the blood flow. Fluid flow is presumed to be laminar, unsteady, two-dimensional, and axisymmetric. The mathematical representation of this system involves expressing the conservation of mass, momentum, and temperature Nadeem and Ijaz [13],

$$\frac{\partial u}{\partial r}+\frac{u}{r}+\frac{\partial w}{\partial z}=0, \tag{2.1}$$

$$\rho_{nf}\left(\frac{\partial u}{\partial t}+u\frac{\partial u}{\partial r}+w\frac{\partial u}{\partial z}\right)=-\frac{\partial p}{\partial r}+\left(\frac{\partial^2 u}{\partial r^2}+\frac{1}{r}\frac{\partial u}{\partial r}-\frac{u^2}{r^2}+\frac{\partial^2 u}{\partial z^2}\right), \tag{2.2}$$

$$\rho_{nf}\left(\frac{\partial w}{\partial t}+u\frac{\partial w}{\partial r}+w\frac{\partial w}{\partial z}\right)=-\frac{\partial p}{\partial z}+\mu_{nf}\left(\frac{\partial^2 w}{\partial r^2}+\frac{1}{r}\frac{\partial w}{\partial r}+\frac{\partial^2 w}{\partial z^2}\right)+g(\rho\gamma)_{nf}(T-T_1), \tag{2.3}$$

$$\left(\frac{\partial T}{\partial t}+u\frac{\partial T}{\partial r}+w\frac{\partial T}{\partial z}\right)=\left(\frac{k_{nf}}{(\rho C_p)_{nf}}\right)\left(\frac{\partial^2 T}{\partial r^2}+\frac{1}{r}\frac{\partial T}{\partial r}+\frac{\partial^2 T}{\partial z^2}\right)+\frac{Q_0}{(\rho C_p)_{nf}}, \tag{2.4}$$

where $u$ and $w$ are radial and axial velocities respectively; $\mu_{nf}$, $\rho_{nf}$, $k_{nf}$ and $\gamma_{nf}$ are viscosity, density, thermal conductivity, coefficient of thermal expansion of nanofluids. $T$ is temperature of fluid, $Q_0$ is constant of heat absorption or heat generation.

The dynamic viscosity $\mu_{nf}$ of the nanofluid is given by Nadeem and Ijaz [13],

$$\mu_{nf}=\frac{\mu_f}{(1-\phi)^{2.5}}.$$

The thermal conductivity ($k_{nf}$), coefficient of thermal expansion ($\gamma_{nf}$) and density ($\rho_{nf}$) of nanofluids is given by Oztop and Abu-Nada [14] and Ajdari *et al*. [2],

$$k_{nf}=k_f\left[\frac{2k_f+k_s-2\phi(k_f-k_s)}{2k_f+k_s+\phi(k_f-k_s)}\right],$$

$$\gamma_{nf}=(1-\phi)\gamma_f+\rho\gamma_s,$$

$$\rho_{nf}=(1-\phi)\rho_f+\rho_s\phi,$$

where $\phi$ is the concentration of nanoparticles, $k_s, \rho_s$ and $\gamma_s$ are thermal conductivity, coefficient of thermal expansion and density of nanoparticles.

**Table 1.** Physical values of blood and nanoparticle are given by Zaman *et al*. [22]

| Parameters | Blood | Cu | Ag |
|---|---|---|---|
| $C_p$ (J/Kg K) | 3594 | 385 | 235 |
| $\rho$ (Kg/m$^3$) | 1063 | 8933 | 10500 |
| $\gamma$ (1/K) | 0.18 | $1.89 \times 10^{-5}$ | $1.67 \times 10^{-5}$ |
| $K$ (W/m K) | 0.492 | 400 | 429 |

## 3. The Stenosis Geometry

The time-dependent geometry of the stenosis is presented as Ikbal *et al*. [9],

$$R(z,t) = \begin{cases} a_1(t)\left\{a - \frac{\tau_m}{2}\left[1 + \cos\left\{\frac{\pi(z-l_1)}{l_0}\right\}\right]\right\}, & d < z < d + 2l_0, \\ aa_1(t), & \text{otherwise}, \end{cases}$$

where $a_1(t) = 1 + K_R \cos(\omega t - \psi)$, $\omega$ is angular frequency, $\psi$ is the phase difference and $K_R$ is a constant; $l_0$ is the center of the stenosis, $l_1$ is the half length of the stenosis region, $\tau_m$ is the maximum height of the stenosis and $a$ is the radius of the artery in non stenotic region. Arterial segment of length 3 cm is considered for this study.

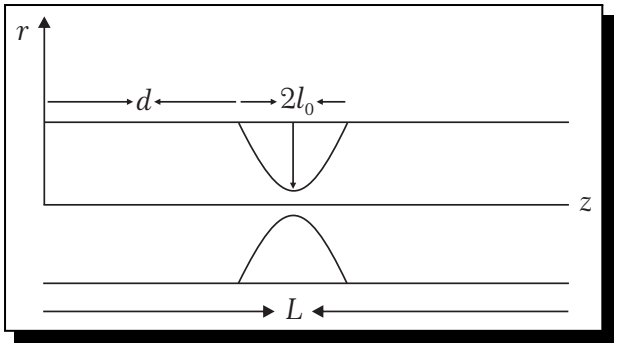


**Figure 1.** The geometry in an stenosed artery

## 4. Boundary Conditions

The velocities at the inlet and outlet of an arterial segment of finite length are taken as

$$u(r,z,t) = 0 \text{ and } w(r,z,t) = \frac{5}{3}\left(1 - \left(\frac{r}{R(z,t)}\right)^3\right) \text{ at } z = 0, \tag{4.1}$$

$$\frac{\partial w(r,z,t)}{\partial z} = 0 = \frac{\partial u(r,z,t)}{\partial z} \text{ at } z = L. \tag{4.2}$$

It is presumed that both radial and axial velocities are initially zero, representing the system at rest and no flow through the artery; consequently, leading to a radial velocity of zero,

$$u(r,z,0) = 0,\ w(r,z,0) = 0,\ T(r,z,0) = 0. \tag{4.3}$$

The gradients of axial velocity, blood temperature, and temperature gradient are considered to be zero. This can be expressed as

$$\frac{\partial w}{\partial r} = 0,\ u(r,z,t) = 0,\ \frac{\partial T}{\partial r} = 0 \text{ on } r = 0. \tag{4.4}$$

At the artery wall, the axial velocity is zero, following the no-slip condition. The fluid temperature is zero, and the radial velocity corresponds to the rate of change in the shape of

the stenosis. This relationship can be expressed as

$$w(r,z,t)=0,\ u(r,z,t)=\frac{\partial R}{\partial t},\ T(r,z,t)=0 \text{ on } r=R(z,t). \tag{4.5}$$

## 5. Numerical Method and Implementation

The governing equations are discretized using a finite-difference scheme with baseline discretization $\Delta x=0.05$, $\Delta z=0.025$ and $\Delta t=1\times10^{-6}$. After implementing a radial coordinate transformation, $x=\frac{r}{R(z,t)}$, equations (2.3) and (2.4) along with boundary conditions (4.1) to (4.5) assume the following form

$$\frac{\partial w}{\partial t}=\frac{1}{R}\left[x\left(w\frac{\partial R}{\partial z}+\frac{\partial R}{\partial t}\right)-u\right]\frac{\partial w}{\partial x}-w\frac{\partial w}{\partial z}+\frac{\mu_{nf}}{\rho_{nf}R^2}\left(\frac{\partial^2 w}{\partial x^2}+\frac{1}{x}\frac{\partial w}{\partial x}\right)-\frac{1}{\rho_{nf}}\frac{\partial p}{\partial z}+g(\gamma)_{nf}(T-T_1), \tag{5.1}$$

$$\frac{\partial T}{\partial t}=\frac{1}{R}\left[x\left(T\frac{\partial R}{\partial z}+\frac{\partial R}{\partial t}\right)-u\right]\frac{\partial T}{\partial x}-T\frac{\partial T}{\partial z}+\left(\frac{k_{nf}}{(\rho C_p)_{nf}}\right)\frac{1}{R^2}\left(\frac{\partial^2 T}{\partial x^2}+\frac{1}{x}\frac{\partial T}{\partial x}\right)+\frac{Q_0}{(\rho C_p)_{nf}}, \tag{5.2}$$

$$u(x,z,t)=0 \text{ and } w(x,z,t)=\frac{5}{3}(1-x^3) \text{ at } z=0, \tag{5.3}$$

$$\frac{\partial w(x,z,t)}{\partial z}=0=\frac{\partial u(x,z,t)}{\partial z} \text{ at } z=L \tag{5.4}$$

$$u(x,z,0)=0,\ w(x,z,0)=0,\ T(x,z,0)=0, \tag{5.5}$$

$$\frac{\partial w}{\partial x}=0,\ u(x,z,t)=0,\ \frac{\partial T}{\partial x}=0 \text{ on } x=0, \tag{5.6}$$

$$w(x,z,t)=0,\ u(x,z,t)=\frac{\partial R}{\partial t},\ T(x,z,t)=0 \text{ on } x=1. \tag{5.7}$$

Equations (5.1) and (5.2) are solved by applying finite difference approximations using central differences

$$\frac{\partial w}{\partial x}=\frac{w^k_{i,j+1}-w^k_{i,j-1}}{2\Delta x},$$

$$\frac{\partial w}{\partial z}=\frac{w^k_{i+1,j}-w^k_{i-1,j}}{2\Delta z},$$

$$\frac{\partial w}{\partial t}=\frac{w^{k+1}_{i,j}-w^k_{i,j}}{\Delta t},$$

$$\frac{\partial^2 w}{\partial x^2}=\frac{w^k_{i,j+1}-2w^k_{i,j}+w^k_{i,j-1}}{(\Delta x)^2},$$

where $x_j=(j-1)\Delta x$, $z_i=(i-1)\Delta z$, $t_k=(k-1)\Delta t$; $\Delta x$ and $\Delta z$ are increments in radial and axial directions, respectively; giving us the equations

$$\begin{aligned}w^{k+1}_{i,j}=w^k_{i,j}+\Delta t\Bigg\{&\frac{-1}{\rho_{nf}}\left(\frac{\partial p}{\partial z}\right)^{k+1}-w^k_{i,j}\left(\frac{w^k_{i+1,j}-w^k_{i-1,j}}{2\Delta z}\right)+\left(\frac{x_j}{R^k_i}w^k_{i,j}\left(\frac{\partial R}{\partial z}\right)^k_i+\frac{x_j}{R^k_i}\left(\frac{\partial R}{\partial t}\right)^k_i-\frac{u^k_{i,j}}{R^k_i}\right)\\&\cdot\left(\frac{w^k_{i,j+1}-w^k_{i,j-1}}{2\Delta x}\right)+\frac{\mu_{nf}}{\rho_{nf}(R^k_i)^2}\left[\frac{w^k_{i,j+1}-2w^k_{i,j}+w^k_{i,j-1}}{(\Delta x)^2}+\frac{1}{x_j}\left(\frac{w^k_{i,j+1}-w^k_{i,j-1}}{2\Delta x}\right)\right]\\&+g(\gamma)_{nf}(T-T_1)\Bigg\},\end{aligned} \tag{5.8}$$

$$T_{i,j}^{k+1} = T_{i,j}^{k} + \Delta t\Big\{T_{i,j}^{k}\Big(\frac{T_{i+1,j}^{k} - T_{i-1,j}^{k}}{2\Delta z}\Big) + \Big(\frac{x_j}{R_i^k}T_{i,j}^{k}\Big(\frac{\partial R}{\partial z}\Big)_i^k + \frac{x_j}{R_i^k}\Big(\frac{\partial R}{\partial t}\Big)_i^k - \frac{u_{i,j}^k}{R_i^k}\Big)\Big(\frac{T_{i,j+1}^{k} - T_{i,j-1}^{k}}{2\Delta x}\Big)$$
$$+\Big(\frac{k_{nf}}{(\rho C_p)_{nf}}\Big)\frac{1}{R_i^k}\Big[\frac{T_{i,j+1}^{k} - 2T_{i,j}^{k} + T_{i,j-1}^{k}}{(\Delta x)^2} + \frac{1}{x_j}\Big(\frac{T_{i,j+1}^{k} - T_{i,j-1}^{k}}{2\Delta x}\Big)\Big] + \frac{Q_0}{(\rho C_p)_{nf}}. \tag{5.9}$$

Equations (5.8) and (5.9) along with boundary conditions (5.3) to (5.7) are solved numerically using MATLAB.

The calculation of blood flow rate and resistance to flow (Resistive Impedance) can be performed using Mazumdar [10] as

$$Q_i^k = 2\pi(R_i^k)^2\int_0^1 x_j w_{i,j}^k\, dx_j, \tag{5.10}$$

$$X_i^k = \frac{\big|L\big(\frac{\partial p}{\partial z}\big)^k\big|}{Q_i^k}. \tag{5.11}$$

The parameter values are assumed to match the physical properties of the proposed geometry for numerical computations as follows:
$d = 0.005\,\text{m}$, $l_0 = 0.01\,\text{m}$, $L = 0.03\,\text{m}$, $a = 0.0008\,\text{m}$, $f_p = 1.2\,\text{Hz}$, $\mu = 0.035\,\text{P}$, $\tau_m = 0.2\,\text{a}$, $A_0 = 100\,\text{Kg}\,\text{m}^{-2}s^{-2}$, $A_1 = 0.2A_0$.

The numerical model developed in the present study was validated by comparing its results with Ali *et al*. [5], Changdar and De [7] and Sankar *et al*. [17]. The maximum axial velocity in the simulations is observed to be $w_{\max} = 0.4$ cm/s. Consequently, the *Courant–Friedrichs–Lewy* (CFL) number is

$$\text{CFL} = \frac{w_{\max}\Delta x}{\Delta x} \approx 8\times 10^{-8} \tag{5.12}$$

which of magnitude below unity, and therefore, confirms the convective stability of the explicit time integration.

The finite-difference solver was subjected to grid and time-step independence testing. Refining the grid spacing $(\Delta x, \Delta y)$ and time increment $(\Delta t)$ by a factor of two resulted in less than 1% variation in peak axial velocity, volumetric flow rate, and resistive impedance, confirming grid-independent and time-independent solutions. The CFL number, computed using Equation (5.12), confirmed numerical stability of the explicit scheme. The observed convergence behavior is consistent with the theoretical second-order accuracy of the spatial discretization. The model's velocity and impedance trends also show excellent qualitative agreement with those reported in the above finite-difference-based studies, validating the robustness of the present computational approach for predicting hybrid nanoparticle-assisted blood flow in stenosed human arteries.

## 6. Results and Discussion

Radial variation of axial velocity for pure blood, in the presence of Cu NP's and Cu–Ag NP's is presented in Figure 2. It is observed that the axial velocity increases in the presence of nanoparticles. This can be related to reduction in the viscosity gradient of blood due to temperature difference created by presence of these nanoparticles. Figure 2 also show that presence of Cu–Ag hybrid nanoparticles result in a relatively higher rise in the axial velocity as compared to Cu nanoparticles. This can be associated to higher thermal conductivity of Ag as

compared to Cu. In addition, inclusion of a hybrid nanoparticle results in relatively improved momentum of the fluid due the difference in their densities.

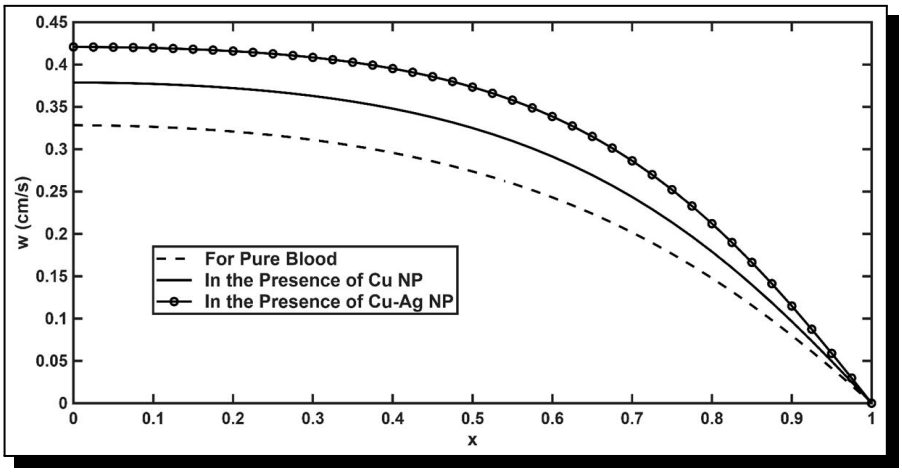


**Figure 2.** Radial variation of axial velocity

Figures 3-4 represent the axial variation of axial velocity and the flow rate for pure blood, in the presence of Cu and Cu–Ag nanoparticles. The result indicate that the axial velocity and flow rate increases significantly after insertion of Cu and Cu–Ag nanoparticles. Although the flow pattern is similar, it is observed that insertion of Cu–Ag nanoparticles have a higher influence in increasing the axial velocity of blood as compared to Cu nanoparticles. The result also suggest that the velocity profiles are highly skewed in the absence of nanoparticles. When blood is augmented by adding nanoparticles, the peak velocity is observed to reduce and the velocity profiles are relatively smoother. Figure 3 shows that the range of variation for axial variation is much smaller when the fluid is augmented with nanoparticles. While the range of variation in axial velocity for blood in absence of nanoparticles is 0.045 cm/s, the range of variation in presence of Cu nanoparticles and Cu–Ag nanoparticles is 0.032 cm/s and 0.028 cm/s, respectively. However, the range of flow rates see a reversal in behavior in each of these three cases.

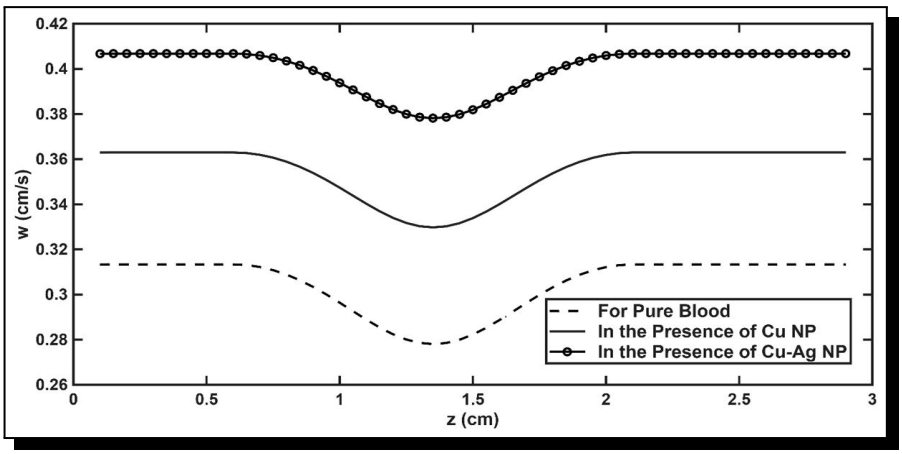


**Figure 3.** Axial variation of axial velocity

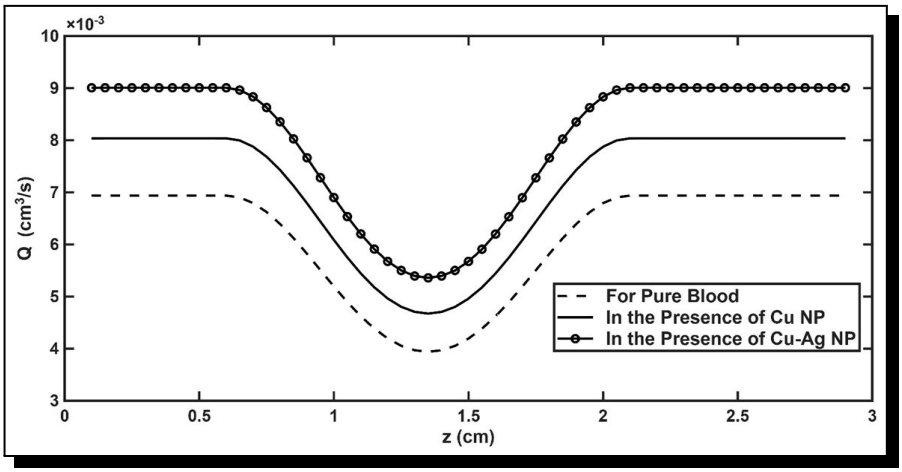


**Figure 4.** Flow rate along axial direction

Figure 4 shows that the range of flow rates for fluid with Cu–Ag and Cu has a range of $3.6 \times 10^{-3}$ cm$^3$/s and $3.3 \times 10^{-3}$ cm$^3$/s, respectively, while the range for the fluid in the absence of nanoparticles is $3.1 \times 10^{-3}$ cm$^3$/s. This suggests that flow rate has a higher variation in case it is augmented with nanoparticles. Results in Figures 3-4 indicate that augmenting fluid with any of these nanoparticles has a significant influence on its flow profiles. Also, insertion of Cu–Ag hybrid nanoparticle has relatively higher influence on the flow profiles as compared to Cu nanoparticles.

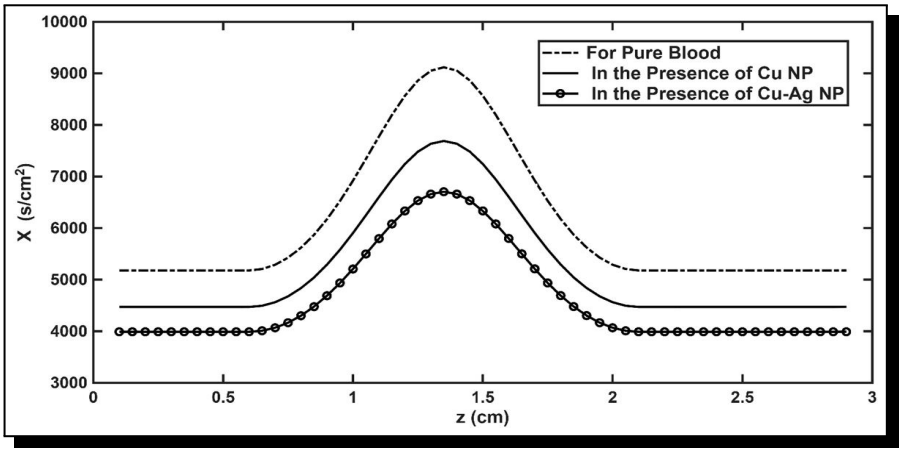


**Figure 5.** Resistance to the flow in axial direction

Resistance to flow in axial direction in the three cases of fluid type viz. blood in absence of nanoparticles, in presence of Cu and in presence of Cu–Ag nanoparticles is presented in Figure 5. It is observed that there is less resistance to blood flow in the affected area after insertion of nanoparticles. In addition, the peak resistance is observed to decrease significantly in the presence of nanoparticles resulting much in smoother blood flow. This can be observed as the flow rate curve tend to show a smoother peak distributed over shorter range after introduction of nanoparticles. In the absence of nanoparticles, a higher resistance is seen in the region affected by stenosis due to a higher shear stress at the wall. The influence of hybrid nanoparticle Cu–Ag on reducing the resistance of flow is observed to be significantly higher as compared to when only Cu nanoparticles are subjected in blood. This is also due to the changes in density of the fluid due to presence of Ag nanoparticles and a higher thermal conductivity.

## 7. Conclusion

Investigation is carried out to study the influence of copper (Cu) nanoparticles and Copper-Silver (Cu–Ag) hybrid nanoparticles on velocity, flow rate and resistive impedance to blood flow in abnormally narrowed arteries due to stenosis. The stenosed artery segment is conceptualized as a cylindrical tube carrying Newtonian fluid to represent the blood flow. Finite difference method is employed to discretize the governing equations and solved numerically. Subsequently, flow profiles are generated through simulation in MATLAB. The findings suggest that both Cu and Cu–Ag nanoparticles have a significant impact on improving blood flow in the affected region. Cu–Ag hybrid nanoparticles stand out as a more effective enhancer of axial velocity, flow rate, and a reducer of resistance in comparison to Cu nanoparticles. Presence of these nanoparticles reduces the peak resistance significantly resulting in a smoother flow rate. Clinically, the findings suggest that the controlled incorporation of hybrid Cu–Ag nanoparticles can beneficially regulate the rheological properties of blood in constricted arteries with potential to facilitate the design of advanced nanofluidic drug carriers and multifunctional therapeutic nanomaterials for cardiovascular treatment. Moreover, the proposed computational framework offers a predictive platform for assessing nanoparticle transport in patient-specific arterial geometries, thereby contributing to the advancement of precision and personalized vascular therapies. Future investigation can include the synthesis of nanoparticles to know the physical-morphological properties of nanoparticles like size, shape and porosity. Various characterization techniques can be used to determine physical–morphological properties of nanoparticles.

## Acknowledgement

The authors are thankful to the Ph.D. supervisor Prof. Neeta D. Kankane for her able guidance.

### Competing Interests

The authors declare that they have no competing interests.

### Authors' Contributions

All the authors contributed significantly in writing this article. The authors read and approved the final manuscript.

## References

**[1]** Z. Abbas, S. Goher and M. S. Shabbir, Analysis of biological mechanism of blood flow containing nanoparticles through an arterial stenosis, *Waves in Random and Complex Media* (2023), 1 – 20, DOI: 10.1080/17455030.2023.2188093.

**[2]** N. Ajdari, C. Vyas, S. L. Bogan, B. A. Lwaleed and B. G. Cousins, Gold nanoparticle interactions in human blood: A model evaluation, *Nanomedicine: Nanotechnology, Biology and Medicine* **13**(4) (2017), 1531 – 1542, DOI: 10.1016/j.nano.2017.01.019.

**[3]** N. S. Akbar, M. Rafiq, T. Muhammad and M. Alghamdi, Biological structural study for the blood casson fluid flow in catheterized diverging tapered stenosed arteries with emerging shaped nanoparticles: Application in drug delivery, *Microfluidics and Nanofluidics* **28**(6) (2024), article number 40, DOI: 10.1007/s10404-024-02735-x.

**[4]** E. A. Algehyne, N. A. Ahammad, M. E. Elnair, M. Zidan, Y. Y. Alhusayni, B. O. El-Bashir, A. Saeed, A. S. Alshomrani and F. Alzahrani, Enhancing heat transfer in blood hybrid nanofluid flow with Ag–$TiO_2$ nanoparticles and electrical field in a tilted cylindrical W-shape stenosis artery: A finite difference approach, *Symmetry* **15**(6) (2023), 1242, DOI: 10.3390/sym15061242.

**[5]** A. Ali, M. Hussain M. S. Anwar and M. Inc, Mathematical modeling and parametric investigation of blood flow through a stenosis artery, *Applied Mathematics and Mechanics* **42** (2021), 1675 – 1684, DOI: 10.1007/s10483-021-2791-8.

**[6]** H. Badfar, Y. M. Saber and A. Sharifi, Numerical simulation of magnetic drug targeting to the stenosis vessel using $Fe_3O_4$ magnetic nanoparticles under the effect of magnetic field of wire, *Cardiovascular Engineering and Technology* **11**(2) (2020), 162 – 175, DOI: 10.1007/s13239-019-00446-x.

**[7]** S. Changdar and S. De, Analytical solution of mathematical model of magnetohydrodynamic blood nanofluid flowing through an inclined multiple stenosed artery, *Journal of Nanofluids* **6**(6) (2017), 1198 – 1205, DOI: 10.1166/jon.2017.1393.

**[8]** A. Hussain, M. N. R. Dar, N. H. Alrasheed, K. Hajlaoui and M. B. B. Hamida, Assessment of heat transfer and the consequences of iron oxide ($Fe_3O_4$) nanoparticles on flow of blood in an abdominal aortic aneurysm, *Heliyon* **9**(7) (2023), e17660, DOI: 10.1016/j.heliyon.2023.e17660.

**[9]** M. A. Ikbal, S. Chakravarty, K. K. Wong, J. Mazumdar and P. K. Mandal, Unsteady response of non-Newtonian blood flow through a stenosed artery in magnetic field, *Journal of Computational and Applied Mathematics* **230**(1) (2009), 243 – 259, DOI: 10.1016/j.cam.2008.11.010.

**[10]** J. Mazumdar, *Biofluid Mechanics*, 2nd edition, World Scientific, Singapore, xvi + 246 pages (2015).

**[11]** S. Y. Motlagh and S. Deyhim, Numerical study of magnetic drug targeting inside the bifurcated channel as a simplified model of right common Iliac artery using Fe3O4–blood magnetic nanofluid, *Iranian Journal of Science and Technology, Transactions of Mechanical Engineering* **47**(1) (2023), 51 – 65, DOI: 10.1007/s40997-022-00507-y.

**[12]** M. Muthtamilselvan and Y. M. G. Hingis, Flow characteristics of gold nanoparticles and microorganisms in a multistenotic artery treated with a catheter, *Australian Journal of Mechanical Engineering* **23**(2) (2023), 326 – 341, DOI: 10.1080/14484846.2023.2290335.

**[13]** S. Nadeem and S. Ijaz, Theoretical analysis of metallic nanoparticles on blood flow through tapered elastic artery with overlapping stenosis, *IEEE Transactions on NanoBioscience* **14**(4) (2015), 417 – 428, DOI: 10.1109/TNB.2015.2389253.

**[14]** H. F. Oztop and E. Abu-Nada, Numerical study of natural convection in partially heated rectangular enclosures filled with nanofluids, *International Journal of Heat and Fluid Flow* **29**(5) (2008), 1326 – 1336, DOI: 10.1016/j.ijheatfluidflow.2008.04.009.

**[15]** S. U. Rahman, R. Ellahi, S. Nadeem and Q. Z. Zia, Simultaneous effects of nanoparticles and slip on Jeffrey fluid through tapered artery with mild stenosis, *Journal of Molecular Liquids* **218** (2016), 484 – 493, DOI: 10.1016/j.molliq.2016.02.080.

**[16]** C. S. K. Raju, H. T. Basha, N. F. M. Noor, N. A. Shah and S.-J. Yook, Significance of body acceleration and gold nanoparticles through blood flow in an uneven/composite inclined stenosis artery: A finite difference computation, *Mathematics and Computers in Simulation* **215** (2024), 399 – 419, DOI: 10.1016/j.matcom.2023.08.006.

**[17]** D. S. Sankar, J. Goh and A. I. M. Ismail, FDM analysis for blood flow through stenosed tapered arteries, *Boundary Value Problems* **2010** (2010), article number 917067, DOI: 10.1155/2010/917067.

**[18]** L. Sarwar and A. Hussain, Flow characteristics of Au-blood nanofluid in stenotic artery, *International Communications in Heat and Mass Transfer* **127** (2021), 105486, DOI: 10.1016/j.icheatmasstransfer.2021.105486.

**[19]** L. Sarwar, A. Hussain, M. B. Riaz and S. Akbar, Modeling and analysis of hybrid-blood nanofluid flow in stenotic artery, *Scientific Reports* **14**(1) (2024), Article number: 5409, DOI: 10.1038/s41598-024-55621-5.

**[20]** T.-Q. Tang, M. Rooman, N. Vrinceanu, Z. Shah and A. Alshehri, Blood flow of Au-nanofluid using Sisko model in stenotic artery with porous walls and viscous dissipation effect, *Micromachines* **13**(8) (2022), 1303, DOI: 10.3390/mi13081303.

**[21]** H. Waqas, U. Farooq, D. Liu, M. Alghamdi, S. Noreen and T. Muhammad, Numerical investigation of nanofluid flow with gold and silver nanoparticles injected inside a stenotic artery, *Materials & Design* **223** (2022), 111130, DOI: 10.1016/j.matdes.2022.111130.

**[22]** A. Zaman, N. Ali and I. Ali, Effects of nanoparticles (Cu (Copper), Silver (Ag)) and slip on unsteady blood flow through a curved stenosed channel with aneurysm, *Thermal Science and Engineering Progress* **5**(2018), 482 – 491, DOI: 10.1016/j.tsep.2018.02.004.